



HAL
open science

Genes and sites under adaptation at the phylogenetic scale also exhibit adaptation at the population-genetic scale

T. Latrille, N. Rodrigue, Nicolas Lartillot

► **To cite this version:**

T. Latrille, N. Rodrigue, Nicolas Lartillot. Genes and sites under adaptation at the phylogenetic scale also exhibit adaptation at the population-genetic scale. 2022. hal-03868900

HAL Id: hal-03868900

<https://hal.science/hal-03868900>

Preprint submitted on 24 Nov 2022

HAL is a multi-disciplinary open access archive for the deposit and dissemination of scientific research documents, whether they are published or not. The documents may come from teaching and research institutions in France or abroad, or from public or private research centers.

L'archive ouverte pluridisciplinaire **HAL**, est destinée au dépôt et à la diffusion de documents scientifiques de niveau recherche, publiés ou non, émanant des établissements d'enseignement et de recherche français ou étrangers, des laboratoires publics ou privés.

GENES AND SITES UNDER ADAPTATION AT THE PHYLOGENETIC SCALE ALSO EXHIBIT ADAPTATION AT THE POPULATION-GENETIC SCALE

T. Latrille^{1,2,3}, N. Rodrigue⁴, N. Lartillot¹

¹Université de Lyon, CNRS, LBBE UMR 5558, Villeurbanne, France

²École Normale Supérieure de Lyon, Université de Lyon, Lyon, France

³Department of Computational Biology, Université de Lausanne, Lausanne, Switzerland

⁴Department of Biology, Institute of Biochemistry, and School of Mathematics and Statistics, Carleton University, Ottawa, Canada

thibault.latrille@ens-lyon.org

September 23, 2022

Abstract

1 Adaptation in protein-coding sequences can be detected from multiple sequence alignments
2 across species, or alternatively by leveraging polymorphism data inside a population. Across
3 species, quantification of the adaptive rate relies on phylogenetic codon models, classically
4 formulated in terms of the ratio of non-synonymous over synonymous substitution rates.
5 Evidence of an accelerated non-synonymous substitution rate is considered a signature of
6 pervasive adaptation. However, because of the background of purifying selection, these
7 models are potentially limited in their sensitivity. Recent developments have led to more
8 sophisticated mutation-selection codon models aimed at making a more detailed quantitative
9 assessment of the interplay between mutation, purifying and positive selection. In this
10 study, we conducted a large-scale exome-wide analysis of placental mammals with mutation-
11 selection models, assessing their performance at detecting proteins and sites under adaptation.
12 Importantly, mutation-selection codon models are based on a population-genetic formalism
13 and thus are directly comparable to McDonald & Kreitman tests at the population level
14 to quantify adaptation. Taking advantage of this relationship between phylogenetic and
15 population genetics, we integrated divergence and polymorphism data across the entire exome
16 for 29 populations across 7 genera, and showed that proteins and sites detected to be under
17 adaptation at the phylogenetic scale are also under adaptation at the population-genetic
18 scale. Altogether, our exome-wide analysis shows that phylogenetic mutation-selection codon
19 models and population-genetic test of adaptation can be reconciled and are congruent, paving
20 the way for integrative models and analyses across individuals and populations.

21 **Keywords** Adaptation · phylogenetic · population genetics · codon models

22 Significance Statement

23 Detecting genes under adaptation represents a key step in the decoding of genomes. Several methods have been
24 proposed, focussing either on the short time scale (population genetics, e.g. human populations), or on the
25 long time scale (phylogenetics, e.g. across mammals). However, the accuracy of these methods is still under
26 debate, and it is still unclear whether the signatures of adaptation are congruent across evolutionary scales. In
27 this study, using novel phylogenetic methods and gathering genome data across and within species, we show
28 that the signatures of adaptation at the phylogenetic and population-genetic scales can be reconciled. While
29 providing a mutual confirmation of the two approaches, our work paves the way for further methodological
30 integration between micro- and macro-evolutionary genomics.

31 Introduction

32 Present-day genetic sequences are informative of populations' past evolutionary history and can carry
33 signatures of selection at different scales. One main goal of molecular evolution is to disentangle and quantify
34 the intensity of neutral, adaptive and purifying evolution acting on sequences, leveraging variations in
35 sequences between and within species. Theoretically, in order to detect adaptive evolution, one must have
36 data where part of the sequence is known to be under a neutral regime, which can be used as a null model.
37 In the case of protein-coding DNA sequences, synonymous sites are usually taken as proxies for neutral sites,
38 although there are instance where they are indeed under selection[1–3]. Non-synonymous mutations, on the
39 other hand, might be under a mixture of varying degrees of adaptive and purifying selection. Contrasting
40 synonymous and non-synonymous changes, two different types of methods have emerged to quantify both
41 positive and purifying selection acting on protein-coding sequences. One method, stemming from phylogeny,
42 uses a multiple sequence alignment comprised of genes from different species and relies on codon models
43 to deduce the selective regime from the patterns of non-synonymous versus synonymous substitutions[4, 5].
44 Starting with the work of McDonald & Kreitman[6], another method, stemming from population genetics,
45 contrasts polymorphism within a population and divergence to a closely related species.

46 At the population-genetic scale, one of the most widely used tests for adaptation relies on the substitutions
47 between two closely related species and polymorphism within one population[6]. Under a strict neutral
48 model (i.e. assuming non-synonymous mutations are either neutral or strongly selected), the ratios of non-
49 synonymous polymorphisms over synonymous polymorphisms (π_N/π_S) and of non-synonymous substitutions
50 over synonymous substitutions (d_N/d_S) are expected to be equal. If, in addition, strongly advantageous
51 mutations occur, they are fixed rapidly in the population, thus contributing solely to divergence but not
52 to polymorphism. As a result, the positive difference between d_N/d_S and π_N/π_S gives an estimate of
53 the adaptive rate $\omega_A = d_N/d_S - \pi_N/\pi_S$ [7]. This simple argument is not strictly valid in the presence of
54 moderately deleterious non-synonymous mutations, which can segregate at substantial frequency in the
55 population without reaching fixation, thus contributing solely to polymorphism, and not to divergence,
56 potentially resulting on an underestimation of the rate of adaptive evolution[8]. Subsequent developments
57 have tried to correct for this effect by relying on an explicit nearly-neutral model[9, 10], so as to estimate
58 the rate of evolution expected in the absence of adaptation (called ω_0) based on polymorphism, and then to
59 compare it with the rate of evolution, $\omega = d_N/d_S$, to get an estimate of the rate of adaptation as $\omega_A = \omega - \omega_0$.

GENES AND SITES UNDER ADAPTATION AT THE PHYLOGENETIC SCALE ALSO EXHIBIT ADAPTATION AT THE POPULATION-GENETIC SCALE

60 In their current formulation, phylogeny-based methods rely on the ratio of non-synonymous substitutions
61 over synonymous substitutions, called ω [4, 5]. Assuming synonymous mutations are neutral, $\omega > 1$ signals an
62 excess in the rate of non-synonymous substitutions compared to the neutral expectation, indicating that the
63 protein is under adaptive evolution. Conversely, a deficit in non-synonymous substitutions, leading to $\omega < 1$,
64 means the protein is under purifying selection. In practice, proteins are typically under a mix of adaptive
65 and purifying selection dominated by the latter, thus typically leading to an $\omega < 1$ even in the presence of
66 positive selection. At a finer scale, site models can detect a specific site (i) of the sequence with a $\omega^{(i)} > 1$ [11,
67 12]. Site models have the advantage of greater sensitivity and the ability to pinpoint where positive selection
68 acts on the protein. However, even at the level of a single site under recurrent adaptation, not all amino-acids
69 are expected to be adaptive, leading to $\omega^{(i)}$ capturing a mix of adaptive and purifying selection, reducing the
70 sensitivity of test. An alternative approach to detect adaptation would be to rely on an explicit nearly-neutral
71 model as the null against which to detect deviations, similarly to the McDonald & Kreitman test. Recent
72 development in this direction, the so-called phylogenetic mutation-selection models provide a null model
73 by estimating the fitness landscape over amino acid sequences, for each site of the sequence[13–15]. At the
74 mutation-selection balance, the probability for a specific codon to be fixed in the population is proportional
75 to its fitness, and a mutation from a high fitness amino acid towards a low fitness amino acid will have a
76 small probability of fixation, genuinely accounting for purifying selection. Conversely, only nearly-neutral
77 mutations between high fitness amino acids will tend to be permitted by the model, allowing for the explicit
78 calculation of the nearly-neutral rate of non-synonymous substitutions at mutation-selection balance, called
79 ω_0 [16, 17]. By contrasting ω estimated by ω -based codon models and ω_0 calculated from mutation-selection
80 models, one can hope to extract the rate of adaptation $\omega_A^{\text{phy}} = \omega - \omega_0$.

81 Interestingly, the rate of adaptation is directly comparable between phylogenetic and population-genetic
82 methods since both seek a deviation of ω from a nearly-neutral null model, estimated with mutation-selection
83 models in phylogenetic context (ω_0) or from standing polymorphism in a population-genetic context (π_N/π_S).
84 This raises the question whether the two signals of adaptation are correlated, thus representing a unique
85 opportunity to confront phylogeny-based and population-based methods. These two methods work over
86 very different time scales, for that reason, they might be capturing different signals: long-term evolutionary
87 Red-Queen for phylogeny-based methods versus events of adaptation in specific lineages for population-based
88 methods. Nonetheless, we expect sites and proteins under long-term evolutionary Red-Queen regimes to
89 maintain their signal of adaptation in several independent lineages for which the McDonald & Kreitman test
90 is applied.

91 Accordingly, in this study, we first applied ω -based and mutation-selection codon models to whole exome
92 data from placental mammals, so as to quantify the rate ω_A^{phy} for each site and protein and detect signatures
93 of adaptive evolution at the phylogenetic scale. Then, we developed a pipeline integrating (and aligning)
94 divergence and polymorphism data across the entire exome for 29 populations across 7 genera, namely *Equus*,
95 *Canis*, *Bos*, *Capra*, *Ovis*, *Chlorocebus* and *Homo*. Finally, using this pipeline, we assessed the congruence
96 between the phylogeny-based and population-based approaches, by testing if the group of sequences detected
97 with a high rate of adaptation in the phylogeny-based method also displays a high rate of adaptation according
98 to the population-based method.

GENES AND SITES UNDER ADAPTATION AT THE PHYLOGENETIC SCALE ALSO EXHIBIT ADAPTATION AT THE POPULATION-GENETIC SCALE

99 Results

100 Detecting genes and sites under adaptation

101 We derived a two-step approach (see methods), which we applied to a set of alignments of orthologous genes
102 at the scale of placental mammals. The d_N/d_S estimated by the site model (ω) is plotted against the d_N/d_S
103 predicted by the nearly-neutral mutation-selection model (ω_0) for genes (scatter plot in fig. 1A) and sites
104 (density plot in fig. 1B). An excess of ω relative to ω_0 is a typical signature of ongoing positive selection[17,
105 18]. Accordingly, genes, or sites, were considered to be under an adaptive regime (in red) if the value of their
106 ω is higher than that of their ω_0 , with non-overlapping 95% posterior credibility intervals. This procedure
107 retrieved 822 out of 14,509 genes, which are putatively under a long-term evolutionary Red-Queen regime. At
108 the site level, the nearly-neutral assumption appears to be rejected for 104,129 out of 8,895,374 sites. Of note,
109 this selection procedure is not meant as a routine statistical test, but only as an enrichment procedure, for
110 the needs of the subsequent analysis shown below. In practice, this selection is likely to be conservative and
111 to have a rate of false discovery of the order of 1% at the gene-level, and 5% at the site-level (see methods).

112 Of note, selection based on $\omega > \omega_0$ is more sensitive than based on the commonly used criterion of $\omega > 1$,
113 since ω_0 is always lower than 1 by definition[16]. Thus, we can uncover sites under adaptation ($\omega > \omega_0$) with
114 a mean ω lower than 1 (29,543 sites in fig. 1C). These sites could not have been detected by ω -based codon
115 models relying on the criterion that $\omega > 1$. At the gene level, only two genes have an estimated $\omega > 1$, such
that this distinction is not relevant.

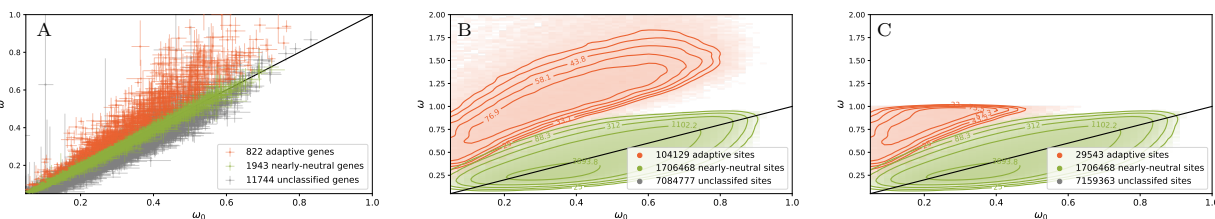


Figure 1: Detection of protein-coding sequences ongoing adaptation at the phylogenetic scale. ω estimated by the site model against ω_0 calculated by the mutation-selection model. Scatter plot of 14,509 genes in panel A, with 95% bayesian credible interval ($\alpha = 0.05$). Density plot of sites in panel B and C. Genes or sites are then classified whether they detected as adaptive ($\omega > \omega_0$ in red) or nearly-neutral ($\omega \simeq \omega_0$ in green). In panel C, the set of sites detected exclusively by mutation-selection codon models have a mean $\omega < 1$.

116

117 Ontology enrichment tests

118 Next, we investigated whether the genes classified as adaptive ($\omega > \omega_0$) showed enrichment in specific ontology
119 terms. Thus, we performed 775 instances of Fisher's exact test to estimate ontology enrichment by contrasting
120 with genes in the control group, not classified as adaptive. 42 ontologies are observed with a p-value (p_v)
121 corrected for multiple comparison (Holm-Bonferroni correction, p_v^{adj}) lower than the risk $\alpha = 0.05$ (see
122 table S1). At a finer scale, we weighted genes by their proportion of sites considered under adaptation with
123 a ω -based site model ($\omega > 1$, see table S2) or with a mutation-selection model ($\omega > \omega_0$, see table S3). For
124 each ontology, the proportion of sites under adaptation is compared between the set of genes sharing this
125 given ontology and the rest of the genes (Mann-Whitney U test). The statistical test based on the the first

GENES AND SITES UNDER ADAPTATION AT THE PHYLOGENETIC SCALE ALSO EXHIBIT ADAPTATION AT THE POPULATION-GENETIC SCALE

126 criterion ($\omega > 1$) is correlated with ontologies related to immune processes, while the statistical test based on
 127 the the second criterion ($\omega > \omega_0$) is also correlated with ontologies related to the external membrane and
 128 cellular adhesion.

129 **Congruence between phylogeny- and population-based methods**

130 Finally, we investigated whether the phylogeny-based and the population-based methods give congruent
 131 results in terms of detection of adaptive evolution (fig. 2). To do so, population genomic data were collected
 132 for 29 populations across 7 genera. For each population, ω_A as proposed by McDonald & Kreitman (MK)[6]
 133 was computed on the concatenate of the 822 genes classified as adaptive by the phylogeny-based method
 134 (red dots in fig. 2 and 3). This result was compared to a null distribution obtained by computing ω_A over
 135 sets of 822 genes that were randomly sampled (1,000 replicates) among the genes classified as nearly-neutral
 136 according to the mutation-selection model (green violins in fig. 2 and 3). Importantly, the terminal lineages
 137 over which the population-genetic method was applied were not included in the phylogenetic analysis. As a
 138 result, the two methods are working on entirely non-overlapping compartments of the evolutionary history
 139 across mammals. For all 29 populations, the ω_A estimated by the population-genetic method was significantly
 140 higher for the putatively adaptive gene-set than for the putatively nearly-neutral gene sets of the same size (at
 141 a risk $\alpha = 0.05$ corrected for multiple testing, Holm-Bonferroni correction). There is thus a good qualitative
 142 agreement between the two methods as to what they capture and interpret as positive selection at the gene
 143 level.

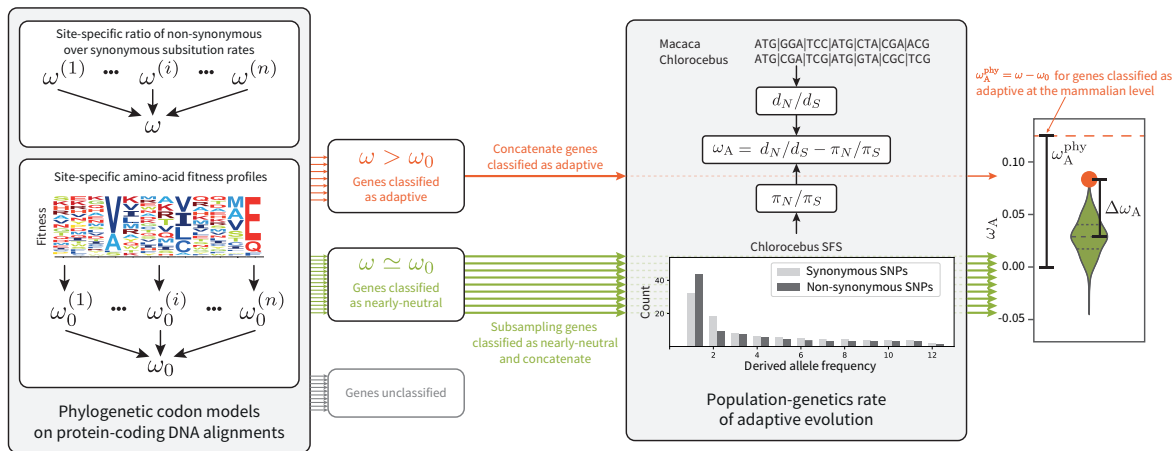


Figure 2: Integrating divergence and polymorphism for the detection of adaptation. At the phylogenetic level, ω (classical codon models) and ω_0 (mutation-selection codon models) are computed from protein-coding DNA alignments, allowing to classify genes into adaptive (in red) and nearly-neutral (in green) regime. At the population-genetic level, for each population, ω_A is computed on the concatenate of genes classified as under adaptation. The result is compared to the empirical null distribution of ω_A in each population, obtained by randomly sampling (1,000 replicates) a subset under a nearly-neutral regime.

144 The same procedure was applied at a finer scale with sites instead of genes. For each population, ω_A was
 145 computed on the concatenate of the 104,129 sites classified as adaptive by the phylogeny-based method, and
 146 compared to the empirical null distribution (fig. 3B) and table 1. Out of 29 populations, 24 have an ω_A
 147 estimated by the population-genetic method significantly higher for the putatively adaptive site-set than

GENES AND SITES UNDER ADAPTATION AT THE PHYLOGENETIC SCALE ALSO EXHIBIT ADAPTATION AT THE POPULATION-GENETIC SCALE

148 for the putatively nearly-neutral site-sets of the same size taken at random (at a risk $\alpha = 0.05$ corrected for
 149 multiple testing, Holm-Bonferroni correction). Of note, the 5 populations for which the test is not significant
 150 are the human populations.

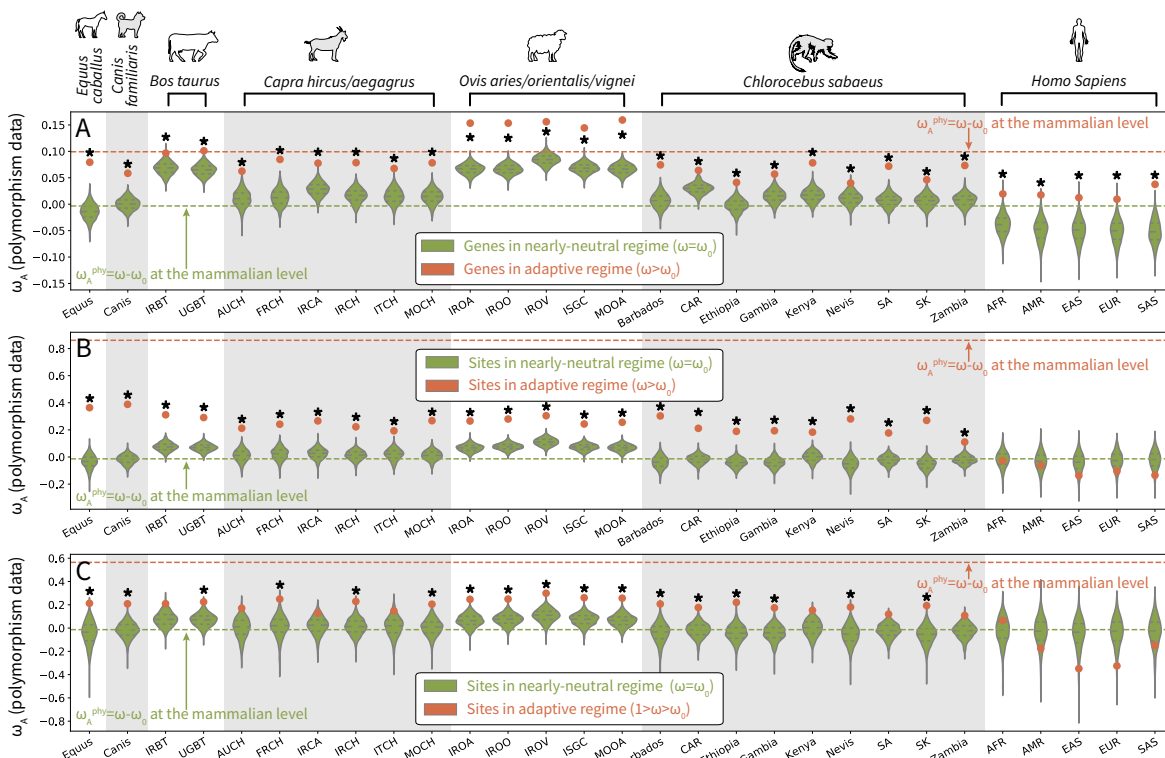


Figure 3: Enrichment of adaptation at the population-genetic scale for 29 populations across 7 genera at the gene (panel A) and site (panels B and C) level. For each population, ω_A is computed on 822 genes (A) and 104,129 sites (B) having a high rate of adaptation at the phylogenetic scale ($\omega > \omega_0$ in red). In panel C, the set of 29,543 sites are detected exclusively by mutation-selection codon models with a mean $\omega < 1$. The result is compared to the empirical null distribution of ω_A , obtained by randomly sampling (1,000 replicates) a subset of genes and sites under a nearly-neutral regime (violin plot in green). * signify that the p_v corrected for multiple comparison (Holm-Bonferroni correction) is lower than the risk $\alpha = 0.05$. The acronym of populations, and the quantitative value of ω_A and p_v are shown in table 1

151 Except for *Equus* and *Humans*, on average, the ω_A returned by MK is positive even for the putatively
 152 nearly-neutral replicates, and significantly so for *Bos* (ω_A in the range 0.65 – 0.68 for genes and site) and
 153 *Ovis* (ω_A in the range 0.66 – 0.84 for genes and sites). This suggests the presence of a background of positive
 154 selection captured by MK methods but not by phylogenetic methods. This background signal could correspond
 155 either to adaptation specifically present in the terminal lineages on which the MK method is applied and
 156 absent over the rest of the mammalian tree, or to low-intensity recurrent positive selection, present over the
 157 tree but nevertheless missed by phylogenetic methods, owing to a lack of sensitivity. Alternatively, part of it
 158 could be an artifact of MK methods, due for example to a recent demographic expansion (*Bos* and *Ovis* are
 159 the two among those analysed by the population-genetic approach showing the highest levels of synonymous
 160 diversity), or to a more general mismatch between short- and long-term effective population size (N_e) [19].

GENES AND SITES UNDER ADAPTATION AT THE PHYLOGENETIC SCALE ALSO EXHIBIT ADAPTATION AT THE POPULATION-GENETIC SCALE

161 Regardless of its exact cause, subtracting this background, so as to compare, not directly the ω_A of the
162 population-genetic method, but the $\Delta\omega_A$ between the putatively adaptive set and the control replicates, to
163 the $\omega_A^{\text{phy}} = \omega - \omega_0$ returned by the phylogenetic method, may give a more meaningful basis for a quantitative
164 comparison between phylogenetic and population-genetic approaches (fig. 2). Of note, across all analyses
165 shown in fig. 3A and B, this population-genetic $\Delta\omega_A$ is always smaller than the phylogenetic ω_A^{phy} . This
166 asymmetry is expected, as a result of a selection bias: the genes of the test set were selected precisely
167 for their high phylogenetic signal, while keeping a blind eye to their population-genetic signal. From this
168 perspective, the ratio $\Delta\omega_A/\omega_A^{\text{phy}}$ can be interpreted as an estimate of the fraction of the total signal captured
169 by the phylogenetic enrichment procedure that is confirmed by MK statistics. This ratio, hereafter called the
170 confirmation rate, is indicated in table 1.

171 At the gene level, the confirmation rate is relatively high, ranging from 30% to up to 90%. At the site level,
172 the confirmation rate is lower (30% on average), which could betray a higher rate of false discovery at the
173 site level, or could be the result of subtle molecular evolutionary processes, such as intermittent adaptation
174 (on some but not on all branches) or within-gene turnover (ongoing adaptation targeting different sites on
175 different branches).

176 After discarding sites with a mean $\omega > 1$, the remaining 29,543 sites classified as being under an adaptive
177 regime have $1 > \omega > \omega_0$ and are specifically discovered by the mutation-selection approach. Since their
178 ω is less than 1, they could not be detected by classical codon models. This raises the question of the
179 empirical value of these findings. Indeed, while mutation-selection methods are more sophisticated and
180 may therefore have a greater sensitivity, they may also be more prone to producing false positives. The
181 phylogenetic/population-genetic confrontation developed here can be used to assess this important point.
182 As shown in (fig. 3C) and table 1, out of 29 populations, for 17 out of the 29 populations that have been
183 analysed, the confirmation rate is significantly positive ($\alpha=0.05$, Holm-Bonferroni correction), and of the
184 order of 10% on average. This importantly suggests the presence of a background of low-intensity positive
185 selection, which is missed by classical codon models, but partially detected by mutation-selection models. In
186 other words, the approach can detect a long-term evolutionary Red-Queen even for a site with $\omega < 1$ that is
187 still under adaptation at the population-genetic scale.

188 Because genes and sites classified as adaptive have a higher ω than genes/sites classified as nearly-neutral,
189 ω_A could simply be higher for genes with higher ω due to this confounding factor. Thus we performed
190 additional experiments where ω is controlled to be the same in the nearly-neutral replicate and the adaptive
191 set of genes (fig. S2-6 and tables S5-9). Additionally, we performed the same experiments with a more
192 stringent risk $\alpha = 0.005$ (10 times greater) to classify genes and sites as adaptive (fig. S7-9 and tables S9-10).
193 Our results are robust to both controlling for ω and with a different threshold to classify genes and sites
194 as adaptive. Finally, we computed ω_A using the software polyDFE[20], which relies on the synonymous
195 and non-synonymous unfolded site-frequency spectra (SFS) to estimate the distribution of fitness effects of
196 mutations (DFE), and the rate of adaptation (fig. S10-17 and tables S11-18). Depending on the underlying
197 assumptions for the shape of the DFE and the definition of ω_A , we observed a wide range of ω_A both for the
198 set of adaptive and nearly-neutral genes/sites. However, the statistical test for the enrichment of ω_A between
199 the set of adaptive and nearly-neutral genes/sites gives results in the same direction whether computed by
200 polyDFE or as McDonald & Kreitman [6] statistic, although the confirmation rate and the associated p_v are
201 different.

GENES AND SITES UNDER ADAPTATION AT THE PHYLOGENETIC SCALE ALSO EXHIBIT ADAPTATION AT THE POPULATION-GENETIC SCALE

Population	Species	π_S	Genes (822)			Sites (104,129)			Sites ($\omega < 1$) (29,543)		
			$\Delta\omega_A$	p_v^{adj}	$\frac{\Delta\omega_A}{\omega_{\text{phy}}}$	$\Delta\omega_A$	p_v^{adj}	$\frac{\Delta\omega_A}{\omega_{\text{phy}}}$	$\Delta\omega_A$	p_v^{adj}	$\frac{\Delta\omega_A}{\omega_{\text{phy}}}$
Diverse (Equus)	Equus caballus	0.002	0.094	0.0*	0.928	0.399	0.0*	0.459	0.258	0.0*	0.446
Diverse (Canis)	Canis familiaris	0.004	0.058	0.0*	0.557	0.406	0.0*	0.463	0.227	0.0*	0.392
Iran (IRBT)	Bos taurus	0.008	0.028	0.020*	0.278	0.237	0.0*	0.272	0.134	0.150	0.231
Uganda (UGBT)	Bos taurus	0.008	0.036	0.0*	0.355	0.222	0.0*	0.254	0.156	0.017*	0.270
Australia (AUCH)	Capra hircus	0.003	0.052	0.0*	0.506	0.202	0.0*	0.230	0.168	0.143	0.290
France (FRCH)	Capra hircus	0.003	0.073	0.0*	0.709	0.220	0.0*	0.250	0.236	0.039*	0.407
Iran (IRCA)	Capra aegagrus	0.004	0.049	0.0*	0.482	0.242	0.0*	0.275	0.108	0.396	0.186
Iran (IRCH)	Capra hircus	0.004	0.062	0.0*	0.610	0.210	0.0*	0.239	0.217	0.017*	0.375
Italy (ITCH)	Capra hircus	0.003	0.052	0.0*	0.511	0.174	0.0*	0.199	0.134	0.308	0.232
Morocco (MOCH)	Capra hircus	0.004	0.064	0.0*	0.626	0.256	0.0*	0.292	0.201	0.0*	0.347
Iran (IROA)	Ovis aries	0.007	0.087	0.0*	0.847	0.199	0.0*	0.228	0.183	0.017*	0.316
Iran (IROO)	Ovis orientalis	0.009	0.087	0.0*	0.848	0.204	0.0*	0.233	0.176	0.0*	0.304
Iran (IROV)	Ovis vignei	0.005	0.072	0.0*	0.697	0.194	0.0*	0.222	0.192	0.0*	0.332
Various (ISGC)	Ovis aries	0.008	0.076	0.0*	0.742	0.171	0.0*	0.195	0.189	0.0*	0.326
Morocco (MOOA)	Ovis aries	0.008	0.093	0.0*	0.905	0.189	0.0*	0.216	0.193	0.0*	0.333
Barbados	Chlorocebus sabaeus	0.003	0.068	0.0*	0.665	0.341	0.0*	0.390	0.248	0.0*	0.430
Central African Republic (CAR)	Chlorocebus sabaeus	0.006	0.034	0.0*	0.334	0.229	0.0*	0.262	0.195	0.0*	0.338
Ethiopia	Chlorocebus sabaeus	0.005	0.044	0.0*	0.425	0.231	0.0*	0.264	0.264	0.0*	0.457
Gambia	Chlorocebus sabaeus	0.005	0.041	0.0*	0.403	0.236	0.0*	0.270	0.217	0.0*	0.375
Kenya	Chlorocebus sabaeus	0.004	0.061	0.0*	0.598	0.181	0.0*	0.207	0.152	0.150	0.264
Nevis	Chlorocebus sabaeus	0.003	0.029	0.020*	0.279	0.332	0.0*	0.380	0.237	0.017*	0.410
South Africa (SA)	Chlorocebus sabaeus	0.006	0.065	0.0*	0.633	0.199	0.0*	0.228	0.142	0.108	0.246
Saint Kitts (SK)	Chlorocebus sabaeus	0.004	0.040	0.0*	0.388	0.324	0.0*	0.371	0.253	0.0*	0.439
Zambia	Chlorocebus sabaeus	0.006	0.066	0.0*	0.642	0.132	0.0*	0.151	0.131	0.150	0.227
African (AFR)	Homo sapiens	0.002	0.059	0.012*	0.568	-0.010	1.000	-0.012	0.089	1.000	0.155
Ad Mixed American (AMR)	Homo sapiens	0.002	0.067	0.006*	0.647	-0.029	1.000	-0.034	-0.141	1.000	-0.244
East Asian (EAS)	Homo sapiens	0.002	0.063	0.006*	0.610	-0.096	1.000	-0.111	-0.296	1.000	-0.513
European (EUR)	Homo sapiens	0.002	0.061	0.015*	0.590	-0.078	1.000	-0.089	-0.289	1.000	-0.500
South Asian (SAS)	Homo sapiens	0.002	0.089	0.0*	0.866	-0.113	1.000	-0.130	-0.111	1.000	-0.193

Table 1: Across 29 populations (rows), table of quantitative value of $\Delta\omega_A$ between the set classified as adaptive and nearly-neutral shown in fig. 3. p_v^{adj} associated to the test are corrected for multiple comparison (Holm–Bonferroni correction, * for $p_v^{\text{adj}} < 0.05$). $\frac{\Delta\omega_A}{\omega_{\text{phy}}}$ is the ratio of $\Delta\omega_A$ at the population-genetic level and the phylogenetic level. π_S is the observed genetic diversity (number of SNPs per site) counted over synonymous sites.

202 Discussion

203 Quantifying the rate of adaptation assumes that we can measure the rate of evolution and more importantly
204 its deviation from a null model of evolution disallowing adaptation. For phylogenetic codon models, this
205 null model of evolution is usually assumed to be neutral evolution and the rate of evolution computed
206 as the ratio of non-synonymous over synonymous substitution rates (ω) is thus compared to 1. We first
207 showed that, at the phylogenetic scale, ω can be compared to its expectation under the mutation-selection
208 model (ω_0), a nearly-neutral model instead of a neutral model of evolution, giving a quantitative estimate
209 of the rate of adaptation as $\omega_A^{\text{phy}} = \omega - \omega_0$. The application of this approach exome-wide across placental
210 mammals suggests that 822 out of 14,509 proteins are under a long-term evolutionary Red-Queen, with
211 ontology terms related to immune processes and the external membrane of cells. Enrichment of ontologies
212 related to immune processes is expected, as found by many studies[12, 21, 22]. However, we also detect an
213 enrichment with ontologies related to the external membrane and cell adhesion, which are the target of virus
214 and parasites. Altogether, the mutation-selection method effectively detects adaptation regardless of the
215 background of purifying selection, and returns reasonable candidates for adaptive evolution. Of note, in its
216 current implementation, and unlike classical codon models[23, 24], the mutation-selection approach does not
217 yet provide a proper and well-calibrated statistical test for calling genes or sites under adaptation with a
218 well-controlled frequentist risk. This was not a problem in the enrichment analysis conducted in this article,
219 which relies on downstream controls based on random permutations. Nevertheless, the encouraging results
220 obtained here give a motivation for developing such a test, which should then have an increased power to
221 detect adaptation, compared to classical codon models relying on the $\omega > 1$ criterion.

GENES AND SITES UNDER ADAPTATION AT THE PHYLOGENETIC SCALE ALSO EXHIBIT ADAPTATION AT THE POPULATION-GENETIC SCALE

222 At the population-genetic scale, the availability of approaches to detect adaptation[6, 25] raises the
223 question whether the rate of adaptation calculated at the phylogenetic scale as ω_A^{phy} is congruent with the
224 rate calculated at the population genetics scale by McDonald & Kreitman (MK)[6] as $\omega_A = d_N/d_S - \pi_N/\pi_S$.
225 In this light, the set of genes and sites detected to be under adaptation at the phylogenetic scale showed
226 a significant increase in ω_A such as inferred by population-based method (29 populations across 7 genera).
227 Quantitatively, about 30% to 90% of the signal detected by the phylogeny-based approach is confirmed by the
228 population-based approach. This result is in stark contrast with studies comparing ω -based codon models at
229 the gene level with MK methods, which found that the set of genes detected at different scales does not seem
230 to overlap beyond random expectations[26]. The reasons for this discrepancy are not totally clear. The use of
231 different codon modeling strategies could play a role here. More fundamentally however, our study relies
232 on a large and densely sampled phylogeny with $\simeq 100$ taxa across placental mammals, versus 5 *Drosophila*
233 and 5 *Brassicaceae* in Chen *et al.* [26]. As a result, the phylogenetic aspect of our analysis benefits from an
234 increased power, while being also inherently more focussed on genes characterized by recurrent adaptation
235 over a very large evolutionary scale (i.e. long-term evolutionary Red Queens), for which population-genetic
236 signals of adaptation may be more easily recovered. We thus showed empirically that the mutation-selection
237 codon model provides a null (nearly-neutral) model from which we can disentangle purifying and adaptive
238 evolution. However, our procedure still has some limitations.

239 Mutation-selection codon models assume a constant effective population size while it has been established
240 that its fluctuations has a major effect on selection dynamics[27, 28]. Estimating changes in effective
241 population size in a mutation-selection framework is possible[29], although too computational intensive in its
242 current implementation to be performed genome-wide. Second, epistasis is not modeled while it can have
243 a large effect on the response of the rate of evolution with change in population size[30]. More generally,
244 pervasive epistasis generates an entrenchment of the amino acids[31–33], resulting in a slowing down of the rate
245 evolution[17, 34] or a standstill[35]. Consequently, our estimation of the predicted rate of evolution computed
246 at mutation-selection balance (ω_0) is over-estimated given that epistasis is not taken into account, such that
247 $\omega_A^{\text{phy}} = \omega - \omega_0$ is thus under-estimated. Altogether, we argue that our estimate of ω_A^{phy} is conservative and
248 could be increased by modeling epistasis (although indirectly) within the mutation-selection framework[33].

249 On the other hand, at the population-genetic scale, the greatest limitation to detecting adaptation is the
250 lack of power determined by the genetic diversity since polymorphisms are rare and estimation of π_N/π_S
251 requires to pool many sites for which SNPs are available. Since the effects of mild purifying selection are
252 more pronounced on longer time scales (i.e. mildly deleterious mutations contribute disproportionately to
253 polymorphism, compared to divergence), ω_A as computed by MK can be biased by moderately deleterious
254 mutations[8, 36] and by the change in population size through time[37]. To overcome this bias, model-based
255 approaches relying on the synonymous and non-synonymous site-frequency spectra (SFS) to estimate the
256 distribution of fitness effects of mutations (DFE), so as to account for the contribution of mild selective
257 effects to standing polymorphism, have been developed[9, 20] and are often used[10, 38]. However, the broad
258 range of ω_A estimated on sets of genes/sites classified as nearly-neutral suggests that these models are lacking
259 power, even more than the MK statistic, because of the sparsity of the SFS. Beside changes in population
260 size biasing the estimation[19], we argue that inferring ω_A using an underlying DFE model is also highly
261 sensitive to assumptions for the shape of the DFE and the definition of ω_A . For example, the value of ω_A is
262 computed as an integral, where the bounds of this integral is debated by different authors[10, 39]. It is thus
263 relatively easy to change the definition of ω_A (fig. S12-15 and tables S13-16) or to constrain the underlying

GENES AND SITES UNDER ADAPTATION AT THE PHYLOGENETIC SCALE ALSO EXHIBIT ADAPTATION AT THE POPULATION-GENETIC SCALE

264 DFE (fig. S12-17 and tables S13-18) to obtain a wide range of ω_A on the same dataset. Taken together,
265 we argue that comparing ω_A to 0 is not a robust test for adaptation. Instead, ω_A for a particular genomic
266 region of interest should be compared to other genomic regions for which the nearly-neutral evolution is not
267 rejected, and the difference $\Delta\omega_A$ should be compared to 0, as done in this study. More generally, our empirical
268 analysis emphasizes the limitations of, and the difficulties raised by, the model-based population-genetic
269 approaches. In this respect, further exploring the congruence (or lack thereof) between phylogenetic and
270 population-genetic approaches will represent a useful asset to clarify those delicate problems, given that
271 similar benefits are also expected on the side of phylogenetic approaches, which are far from immune from
272 methodological limitations.

273 More broadly on a theoretical level, this work leverages a specific overlap between phylogenetic and
274 population genetics, namely that the rate of adaptation ω_A^{phy} in phylogenetic codon models and ω_A in the MK
275 test should theoretically be directly comparable. Based on this theoretical relationship, our study is paving
276 the way for studies and methods augmenting molecular polymorphism data within species with information
277 about divergence data between species[40], and by assessing empirically the relationship between phylogenetic
278 and population genetics[41]. In this light, mutation-selection models at the phylogenetic scale can play a dual
279 role: pinpointing genes and sites under adaptation ($\omega_A^{\text{phy}} > 0$), and also seeking the genomic region for which
280 the nearly-neutral theory is not rejected ($\omega_A^{\text{phy}} \simeq 0$).

281 Methods

282 Phylogenetic dataset

283 Protein-coding DNA sequences alignments in placental mammals and their corresponding gene trees were
284 extracted from the [OrthoMaM](#) database, containing 116 mammalian reference sequences in v10c[42–44].
285 Genes located on the X, Y and mitochondrial chromosome were discarded from the analysis, since the number
286 of polymorphism, necessary in population-based method, is expected to be different on these sequences.
287 Additionally, sequences from the species for which polymorphism are available, as well as their sister species
288 have been discarded from the analysis to ensure independence between the data used in the phylogenetic
289 and population-genetic method. Altogether, we analyzed 14,509 protein-coding DNA sequences alignment
290 containing at most 87 reference sequences of placental mammals.

291 Adaptation in phylogeny-based method

292 Classical codon models estimates a parameter $\omega = d_N/d_S$, namely the ratio of the non-synonymous over
293 the synonymous substitution rates[4, 5]. In the so-called site models, ω is allowed to vary across sites[11,
294 45]. In *Bayescode*, site-specific $\omega^{(i)}$ (fig. 1B, y-axis) are independent identically distributed from a gamma
295 distribution[46]. In a second step, the average over sites is calculated, giving estimates of ω for each
296 protein-coding sequence (fig. 1A, y-axis).

297 In contrast, mutation-selection models assume that the protein-coding sequence is at mutation-selection
298 balance under a fixed fitness landscape, which is itself characterized by a fitness vector over the 20 amino
299 acid at each site[13–15]. Mathematically, the rate of non-synonymous substitution from codon a to codon b
300 ($q_{a \rightarrow b}^{(i)}$) at site i of the sequence is equal to the rate of mutation from the underlying DNA change ($\mu_{a \rightarrow b}$)
301 multiplied by the scaled probability of fixation of the mutation ($\mathbb{P}_{a \rightarrow b}^{(i)}$). Crucially, the probability of fixation

GENES AND SITES UNDER ADAPTATION AT THE PHYLOGENETIC SCALE ALSO EXHIBIT ADAPTATION AT THE POPULATION-GENETIC SCALE

302 depends on the difference of scaled fitness between the amino acid encoded by the mutated codon ($F_b^{(i)}$) and
 303 the fitness of the amino acid encoded by the original codon ($F_a^{(i)}$) of site i [47, 48]. Altogether, the rate of
 304 substitution from codon a to b at a given site i is:

$$q_{a \rightarrow b}^{(i)} = \mu_{a \rightarrow b} P_{a \rightarrow b}^{(i)} = \mu_{a \rightarrow b} \frac{F_b^{(i)} - F_a^{(i)}}{1 - e^{F_a^{(i)} - F_b^{(i)}}}. \quad (1)$$

305 Fitting the mutation-selection model on a sequence alignment leads to an estimation of the mutation rate
 306 matrix (μ) as well as the 20 amino acid fitness landscape ($F^{(i)}$) at each site i . From these parameters, one
 307 can compute $\omega_0^{(i)}$ (fig. 1B, x-axis), the site-specific rate of non-synonymous over synonymous substitution at
 308 the mutation-selection balance:

$$\omega_0^{(i)} = \frac{\sum_{a \in \mathcal{C}} \sum_{b \in \mathcal{N}_a} \pi_a^{(i)} q_{a \rightarrow b}^{(i)}}{\sum_{a \in \mathcal{C}} \sum_{b \in \mathcal{N}_a} \pi_a^{(i)} \mu_{a \rightarrow b}}, \quad (2)$$

where \mathcal{C} is the set all the possible codons (61 by discarding stop codons), $\pi_a^{(i)}$ is the equilibrium frequency
 of codon a at site i , and \mathcal{N}_a is the set of codons that are non-synonymous to a [16, 17]. The equilibrium
 frequency of codon a at site i is the product of the nucleotide frequencies at its three positions and the scaled
 Wrightian fitness of the amino acid ($F_a^{(i)}$):

$$\pi_a^{(i)} = \frac{\sigma_{a[1]} \sigma_{a[2]} \sigma_{a[3]} e^{F_a^{(i)}}}{\sum_{b=1}^{61} \sigma_{b[1]} \sigma_{b[2]} \sigma_{b[3]} e^{F_b^{(i)}}}, \quad (3)$$

309 where $\sigma_{a[j]} \in \{A, T, C, G\}$ is the equilibrium frequency (given by the mutational matrix) of the nucleotide
 310 at position $j \in \{1, 2, 3\}$ of codon a . In a second step, the average over sites is calculated, giving estimates
 311 of ω_0 for each protein-coding sequences (fig. 1A, x-axis). Under the assumption that the protein is under a
 312 nearly-neutral regime, the calculated ω_0 (mutation-selection model) and the estimated ω (site model) should
 313 be the same[16].

314 We ran the Bayesian software *BayesCode* (<https://github.com/ThibaultLatrille/bayescode>) on each
 315 protein-coding DNA alignment[49]. Each Monte-Carlo Markov-Chain (MCMC) is run during 2,000 points,
 316 with a burn-in of 1,000 points, to obtain the posterior mean of ω and ω_0 across the MCMC, as well as the 95%
 317 posterior credibility interval for genes and sites. Genes and sites classified under an adaptive regime (in red)
 318 are rejecting the nearly-neutral assumption such that the lower bound for the credible interval of ω ($\alpha = 0.05$)
 319 is above the upper bound of the credible interval of ω_0 ($\alpha = 0.05$), meaning that the value of their ω is higher
 320 than that of their ω_0 . Because this is a unilateral test ($\omega > \omega_0$) and the two credible interval are independent,
 321 the risk is $(\alpha/2)^2 = 0.025^2 = 0.000625$ for each test. Empirically, the nearly-neutral assumption appears to
 322 be rejected for 822 out 14,509 genes, while $0.000625 \times 14,509 \simeq 9$ genes are expected due to the multiple
 323 testing, suggesting a $9/822 \simeq 1\%$ rate of false positive at the gene level. At the site level, the nearly-neutral
 324 assumption appears to be rejected for 104,129 out of 8,895,374 sites, while $0.000625 \times 8,895,374 \simeq 5,560$ are
 325 expected due to the multiple testing, suggesting a $5,560/104,129 \simeq 5\%$ rate of false positive at the site level.
 326 Genes and sites are classified under a nearly-neutral regime (in green) if the average ω is within the credible
 327 interval of the ω_0 , and respectively the average ω_0 is also within the credible interval of ω , meaning $\omega = \omega_0$.
 328 Additionally, the set of sites detected exclusively by mutation-selection codon models have a mean $\omega < 1$.
 329 Genes and sites that do not fall in any of these categories are considered unclassified.

GENES AND SITES UNDER ADAPTATION AT THE PHYLOGENETIC SCALE ALSO EXHIBIT ADAPTATION AT THE
POPULATION-GENETIC SCALE

330 **Polymorphism dataset**

331 Each SNP (chromosome, position, strand) in the focal species was matched to its relative position (chromosome,
332 position, strand) in the protein-coding DNA alignment by first converting the genomic positions to relative
333 position in the coding sequence (CDS) using gene annotation files (GTF format) downloaded from Ensembl
334 (ensembl.org). We then verified that the SNP downloaded from Ensembl were matching the reference in the
335 CDS (FASTA format). Second, the relative position in the CDS was converted to position in the multiple
336 sequence alignment (containing gaps) from OrthoMaM database[42–44] by doing a global pairwise alignment,
337 using the Biopython function pairwise2, between the CDS fasta and the sequence found in the alignment.
338 This conversion from genomic position to position in the alignment is only possible if the assembly used for
339 SNP calling is the same as the one used in the alignment, the GTF annotations and the FASTA sequences.

340 We retrieved the genetic variants representing the population level polymorphism from the following species
341 and respective available datasets: *Equus caballus* (EquCab2 assembly in the EVA study PRJEB9799[50]),
342 *Canis familiaris* (CanFam3.1 assembly in the EVA study PRJEB24066[51]), *Bos taurus* (UMD3.1 assembly
343 in the NextGen project), *Ovis aries* (Oar_v3.1 assembly in the NextGen project), *Capra Hircus* (CHIR1
344 assembly in the NextGen project converted to ARS1 assembly with dbSNP identifiers[52]), *Chlorocebus*
345 *sabaeus* (ChlSab1.1 assembly in the EVA project PRJEB22989[53]), *Homo sapiens* (GRCh38 assembly from
346 the 1000-genome project[54, 55]).

347 Variants not inside genes are discarded at the beginning of the analysis. Insertions and deletions are not
348 analyzed, and only Single Nucleotide Polymorphisms (SNPs) with only one mutant allele are considered.
349 Stop codon mutants are also discarded. For populations containing more than 8 sampled individuals, the
350 site-frequency spectrum (SFS) is subsampled down to 16 chromosomes (8 diploid individuals) without
351 replacement (hyper-geometric distribution) to alleviate the effect of different sampling depth in the 29
352 populations. Moreover, subsampling mitigate the impact of moderately deleterious mutations segregating at
353 low frequency on π_N/π_S , since they are more likely to be discarded than polymorphism segregating at higher
354 frequency. The Snakemake pipeline for integrating polymorphism and divergence data uses custom scripts
355 written in python 3.9.

356 **Rate of adaption in population-based method**

357 The genes and sites classified as under adaptation are concatenated. For each population π_N/π_S is computed
358 as the sum of non-synonymous over synonymous polymorphism on the concatenated SFS. d_N/d_S is computed
359 on the concatenated pairwise alignment between focal and sister species extracted from OrthoMaM, the
360 d_N/d_S count is performed by *yn00*. We considered *Ceratotherium simum simum* as *Equus caballus* sister
361 species; *Ursus maritimus* as *Canis familiaris* sister species; *Bison bison bison* as *Bos taurus* sister species;
362 *Pantholops hodgsonii* as *Ovis aries* sister species; *Pantholops hodgsonii* as *Capra Hircus* sister species; *Macaca*
363 *mulatta* as *Chlorocebus sabaeus* sister species and finally we considered *Pan troglodytes* as *Homo sapiens* sister
364 species. Altogether, $\omega_A = d_N/d_S - \pi_N/\pi_S$ is thus computed for each population on genes and sites classified
365 as under adaptation. The result is compared to the empirical null distribution of ω_A , obtained by randomly
366 sampling (1,000 sampling replicates) a subset of genes/sites classified as nearly-neutral.

367 Other methods to compute ω_A such as polyDFE[20] are also used (eq. 3-20 in supplementary materials),
368 which relies on the synonymous and non-synonymous unfolded site-frequency spectra (SFS) to estimate the

GENES AND SITES UNDER ADAPTATION AT THE PHYLOGENETIC SCALE ALSO EXHIBIT ADAPTATION AT THE
POPULATION-GENETIC SCALE

369 distribution of fitness effects of mutations (DFE), and the rate of adaptation. In polyDFE, GammaExpo
370 models the fitness effect of weakly deleterious non-synonymous mutations as distributed according to a
371 negative Gamma and the fitness effect of weakly advantageous mutations are distributed exponentially. This
372 method is an extension of the methods introduced by Eyre-Walker and collaborators[9, 56]. Unfolded SFSs
373 are obtained by polarizing SNPs using the 3 closest outgroups found in the OrthoMam alignment with est-usfs
374 v2.04[57].

375 1 Data availability

376 The data underlying this article are available at [10.5281/zenodo.7107234](https://doi.org/10.5281/zenodo.7107234). Scripts and instructions necessary
377 to reproduce the empirical experiments on the original dataset or with user-specified datasets is available at
378 <https://github.com/ThibaultLatrille/AdaptaPop>.

379 2 Acknowledgements

380 We gratefully also acknowledge the help of Nicolas Galtier and Julien Joseph for their advice and review
381 concerning this manuscript. This work was performed using the computing facilities of the CC LBBE/PRABI.
382 This study makes use of data generated by the NextGen Consortium. The European Union’s Seventh
383 Framework Programme (FP7/2010-2014) provided funding for the project under grant agreement no 244356 -
384 “NextGen”. Funding: Université de Lausanne. Agence Nationale de la Recherche, Grant ANR-15-CE12-0010-01
385 / DASIRE. Agence Nationale de la Recherche, Grant ANR-19-CE12-0019 / HotRec.

386 3 Author information

387 TL, NR and NL designed the study. TL gathered and formatted the data and conducted the analyses with
388 BayesCode using scripts in Python and pipeline in Snakemake. TL, NR and NL contributed to the writing of
389 the manuscript.

390 References

- 391 1. Duret, L. & Mouchiroud, D. Expression Pattern and, Surprisingly, Gene Length Shape Codon Usage in
392 Caenorhabditis, Drosophila, and Arabidopsis. *Proceedings of the National Academy of Sciences of the*
393 *United States of America* **96**, 4482–4487 (Apr. 1999).
- 394 2. Duret, L. Evolution of Synonymous Codon Usage in Metazoans. *Current Opinion in Genetics &*
395 *Development* **12**, 640–649 (Dec. 1, 2002).
- 396 3. Galtier, N. *et al.* Codon Usage Bias in Animals: Disentangling the Effects of Natural Selection, Effective
397 Population Size, and GC-Biased Gene Conversion. *Molecular Biology and Evolution* **35**, 1092–1103
398 (2018).
- 399 4. Muse, S. V. & Gaut, B. S. A Likelihood Approach for Comparing Synonymous and Nonsynonymous
400 Nucleotide Substitution Rates, with Application to the Chloroplast Genome. *Molecular Biology and*
401 *Evolution* **1**, 715–724 (1994).

GENES AND SITES UNDER ADAPTATION AT THE PHYLOGENETIC SCALE ALSO EXHIBIT ADAPTATION AT THE
POPULATION-GENETIC SCALE

- 402 5. Goldman, N. & Yang, Z. A Codon-Based Model of Nucleotide Substitution for Protein-Coding DNA
403 Sequences. *Molecular Biology and Evolution* **11**, 725–736 (1994).
- 404 6. McDonald, J. H. & Kreitman, M. Adaptative Protein Evolution at Adh Locus in Drosophila. *Nature*
405 **351**, 652–654 (1991).
- 406 7. Smith, N. G. & Eyre-Walker, A. Adaptive Protein Evolution in Drosophila. *Nature* **415**, 1022–1024
407 (Feb. 2002).
- 408 8. Eyre-Walker, A., Keightley, P. D., Smith, N. G. C. & Gaffney, D. Quantifying the Slightly Deleterious
409 Mutation Model of Molecular Evolution. *Molecular Biology and Evolution* **19**, 2142–2149 (2002).
- 410 9. Eyre-Walker, A. & Keightley, P. D. Estimating the Rate of Adaptive Molecular Evolution in the Presence
411 of Slightly Deleterious Mutations and Population Size Change. *Molecular Biology and Evolution* **26**,
412 2097–2108 (2009).
- 413 10. Galtier, N. Adaptive Protein Evolution in Animals and the Effective Population Size Hypothesis. *PLoS*
414 *Genetics* **12**, e1005774 (2016).
- 415 11. Yang, Z., Nielsen, R., Goldman, N. & Pedersen, A.-m. K. Codon-Substitution Models for Heterogeneous
416 Selection Pressure at Amino Acid Sites. *Genetics* **155**, 431–449 (May 2000).
- 417 12. Kosiol, C. *et al.* Patterns of Positive Selection in Six Mammalian Genomes. *PLoS Genetics* **4**, e1000144
418 (2008).
- 419 13. Yang, Z. & Nielsen, R. Mutation-Selection Models of Codon Substitution and Their Use to Estimate
420 Selective Strengths on Codon Usage. *Molecular Biology and Evolution* **25**, 568–579 (2008).
- 421 14. Halpern, A. L. & Bruno, W. J. Evolutionary Distances for Protein-Coding Sequences: Modeling Site-
422 Specific Residue Frequencies. *Molecular Biology and Evolution* **15**, 910–917 (July 1998).
- 423 15. Rodrigue, N. & Philippe, H. Mechanistic Revisions of Phenomenological Modeling Strategies in Molecular
424 Evolution. *Trends in Genetics* **26**, 248–252 (June 2010).
- 425 16. Spielman, S. J. & Wilke, C. O. The Relationship between dN/dS and Scaled Selection Coefficients.
426 *Molecular biology and evolution* **32**, 1097–1108 (2015).
- 427 17. Rodrigue, N. & Lartillot, N. Detecting Adaptation in Protein-Coding Genes Using a Bayesian Site-
428 Heterogeneous Mutation-Selection Codon Substitution Model. *Molecular Biology and Evolution* **34**,
429 204–214 (2017).
- 430 18. Bloom, J. D. Identification of Positive Selection in Genes Is Greatly Improved by Using Experimentally
431 Informed Site-Specific Models. *Biology Direct* **12**, 1–24 (2017).
- 432 19. Rousselle, M., Mollion, M., Nabholz, B., Bataillon, T. & Galtier, N. Overestimation of the Adaptive
433 Substitution Rate in Fluctuating Populations. *Biology Letters* **14**, 20180055 (2018).
- 434 20. Tataru, P. & Bataillon, T. *polyDFE: Inferring the Distribution of Fitness Effects and Properties of*
435 *Beneficial Mutations from Polymorphism Data in Methods in Molecular Biology* 125–146 (Humana Press
436 Inc., 2020).
- 437 21. Enard, D., Cai, L., Gwennap, C. & Petrov, D. A. Viruses Are a Dominant Driver of Protein Adaptation
438 in Mammals. *eLife* **5**, e12469 (2016).
- 439 22. Ebel, E. R., Telis, N., Venkataram, S., Petrov, D. A. & Enard, D. High Rate of Adaptation of Mammalian
440 Proteins That Interact with Plasmodium and Related Parasites. *PLoS Genetics* **13** (ed Read, A. F.)
441 e1007023 (Sept. 2017).

GENES AND SITES UNDER ADAPTATION AT THE PHYLOGENETIC SCALE ALSO EXHIBIT ADAPTATION AT THE POPULATION-GENETIC SCALE

- 442 23. Wong, W. S. W., Yang, Z., Goldman, N. & Nielsen, R. Accuracy and Power of Statistical Methods for
443 Detecting Adaptive Evolution in Protein Coding Sequences and for Identifying Positively Selected Sites.
444 *Genetics* **168**, 1041–1051 (Oct. 1, 2004).
- 445 24. Yang, Z. PAML 4: Phylogenetic Analysis by Maximum Likelihood. *Molecular Biology and Evolution* **24**,
446 1586–1591. pmid: [17483113](#) (Aug. 2007).
- 447 25. Messer, P. W. & Petrov, D. A. Frequent Adaptation and the McDonald–Kreitman Test. *Proceedings of*
448 *the National Academy of Sciences* **110**, 8615–8620 (2013).
- 449 26. Chen, Q. *et al.* Two Decades of Suspect Evidence for Adaptive Molecular Evolution – Negative Selection
450 Confounding Positive Selection Signals. *National Science Review* **9**, nwab217 (Dec. 3, 2021).
- 451 27. Lanfear, R., Kokko, H. & Eyre-Walker, A. Population Size and the Rate of Evolution. *Trends in Ecology*
452 *and Evolution* **29**, 33–41 (Jan. 2014).
- 453 28. Platt, A., Weber, C. C. & Liberles, D. A. Protein Evolution Depends on Multiple Distinct Population
454 Size Parameters. *BMC Evolutionary Biology* **18**, 1–9 (Dec. 2018).
- 455 29. Latrille, T., Lanore, V. & Lartillot, N. Inferring Long-Term Effective Population Size with Muta-
456 tion–Selection Models. *Molecular Biology and Evolution* **38**, 4573–4587 (Oct. 1, 2021).
- 457 30. Latrille, T. & Lartillot, N. Quantifying the Impact of Changes in Effective Population Size and Expression
458 Level on the Rate of Coding Sequence Evolution. *Theoretical Population Biology* **142**, 57–66 (Dec. 1,
459 2021).
- 460 31. Goldstein, R. A. Evolutionary Perspectives on Protein Thermo Dynamics. *International Conference on*
461 *Computational Science* **3039**, 718–727 (2004).
- 462 32. Goldstein, R. A., Pollard, S. T., Shah, S. D. & Pollock, D. D. Nonadaptive Amino Acid Convergence
463 Rates Decrease over Time. *Molecular Biology and Evolution* **32**, 1373–1381 (June 2015).
- 464 33. Goldstein, R. A. & Pollock, D. D. Sequence Entropy of Folding and the Absolute Rate of Amino Acid
465 Substitutions. *Nature Ecology & Evolution* **1**, 1923–1930 (Dec. 2017).
- 466 34. Patel, R., Carnevale, V. & Kumar, S. Epistasis Creates Invariant Sites and Modulates the Rate of
467 Molecular Evolution. *Molecular Biology and Evolution* **39**, msac106 (May 1, 2022).
- 468 35. Youssef, N., Susko, E., Roger, A. J. & Bielawski, J. P. Evolution of Amino Acid Propensities under
469 Stability-Mediated Epistasis. *Molecular Biology and Evolution* **39**, msac030 (Mar. 1, 2022).
- 470 36. Ho, S. Y. W., Phillips, M. J., Cooper, A. & Drummond, A. J. Time Dependency of Molecular Rate
471 Estimates and Systematic Overestimation of Recent Divergence Times. *Molecular Biology and Evolution*
472 **22**, 1561–1568 (2005).
- 473 37. Eyre-Walker, A. Changing Effective Population Size and the McDonald–Kreitman Test. *Genetics* **162**,
474 2017–2024 (2002).
- 475 38. Moutinho, A. F., Bataillon, T. & Dutheil, J. Y. Variation of the Adaptive Substitution Rate between
476 Species and within Genomes. *Evolutionary Ecology* **34**, 315–338 (June 2019).
- 477 39. Tataru, P. & Bataillon, T. polyDFEv2.0: Testing for Invariance of the Distribution of Fitness Effects
478 within and across Species. *Bioinformatics* **35**, 2868–2869 (2019).
- 479 40. Chen, J., Bataillon, T., Glémin, S. & Lascoux, M. Hunting for Beneficial Mutations: Conditioning on
480 SIFT Scores When Estimating the Distribution of Fitness Effect of New Mutations. *Genome Biology*
481 *and Evolution* (2021).

GENES AND SITES UNDER ADAPTATION AT THE PHYLOGENETIC SCALE ALSO EXHIBIT ADAPTATION AT THE POPULATION-GENETIC SCALE

- 482 41. Thorne, J. L., Lartillot, N., Rodrigue, N. & Choi, S. C. *Codon Models as a Vehicle for Reconciling*
483 *Population Genetics with Inter-Specific Sequence Data* in *Codon Evolution: Mechanisms and Models*
484 97–110 (Oxford University Press, 2012).
- 485 42. Ranwez, V. *et al.* OrthoMaM: A Database of Orthologous Genomic Markers for Placental Mammal
486 Phylogenetics. *BMC Evolutionary Biology* **7**, 1–12 (Nov. 2007).
- 487 43. Douzery, E. J. *et al.* OrthoMaM v8: A Database of Orthologous Exons and Coding Sequences for
488 Comparative Genomics in Mammals. *Molecular Biology and Evolution* **31**, 1923–1928 (2014).
- 489 44. Scornavacca, C. *et al.* OrthoMaM V10: Scaling-up Orthologous Coding Sequence and Exon Alignments
490 with More than One Hundred Mammalian Genomes. *Molecular Biology and Evolution* **36** (ed Tamura,
491 K.) 861–862 (Apr. 2019).
- 492 45. Huelsenbeck, J. P., Jain, S., Frost, S. W. D. & Kosakovsky Pond, S. L. A Dirichlet Process Model for
493 Detecting Positive Selection in Protein-Coding DNA Sequences. *Proceedings of the National Academy of*
494 *Sciences* **103**, 6263–6268 (2006).
- 495 46. Lartillot, N., Rodrigue, N., Stubbs, D. & Richer, J. PhyloBayes MPI. Phylogenetic Reconstruction with
496 Infinite Mixtures of Profiles in a Parallel Environment. *Systematic Biology* **62**, 611–615 (2013).
- 497 47. Wright, S. Evolution in Mendelian Populations. *Genetics* **16**, 97–159 (1931).
- 498 48. Fisher, R. A. *The Genetical Theory of Natural Selection* (The Clarendon Press, 1930).
- 499 49. Rodrigue, N., Lartille, T. & Lartillot, N. A Bayesian Mutation-Selection Framework for Detecting Site-
500 Specific Adaptive Evolution in Protein-Coding Genes. *Molecular Biology and Evolution* **38**, 1199–1208
501 (Mar. 2021).
- 502 50. Al Abri, M. A., Holl, H. M., Kalla, S. E., Sutter, N. B. & Brooks, S. A. Whole Genome Detection of
503 Sequence and Structural Polymorphism in Six Diverse Horses. *PLoS ONE* **15**, e0230899 (Apr. 9, 2020).
- 504 51. Jagannathan, V., Drögemüller, C., Leeb, T. & Consortium (DBVDC), D. B. V. D. A Comprehensive
505 Biomedical Variant Catalogue Based on Whole Genome Sequences of 582 Dogs and Eight Wolves.
506 *Animal Genetics* **50**, 695–704 (2019).
- 507 52. Sherry, S. T. *et al.* dbSNP: The NCBI Database of Genetic Variation. *Nucleic Acids Research* **29**,
508 308–311 (Jan. 1, 2001).
- 509 53. Svardal, H. *et al.* Ancient Hybridization and Strong Adaptation to Viruses across African Vervet Monkey
510 Populations. *Nature Genetics* **49**, 1705–1713 (Dec. 2017).
- 511 54. Consortium, T. 1. G. P. An Integrated Map of Genetic Variation from 1,092 Human Genomes. *Nature*
512 **491**, 56–65 (2012).
- 513 55. The 1000 Genomes Project Consortium. A Global Reference for Human Genetic Variation. *Nature* **526**,
514 68–74 (2015).
- 515 56. Eyre-Walker, A., Woolfit, M. & Phelps, T. The Distribution of Fitness Effects of New Deleterious Amino
516 Acid Mutations in Humans. *Genetics* **173**, 891–900 (2006).
- 517 57. Keightley, P. D. & Jackson, B. C. Inferring the Probability of the Derived vs the Ancestral Allelic State
518 at a Polymorphic Site. *Genetics* **209**, 897–906 (July 2018).